Int. J. Electrochem. Sci., 7 **(2012)** 5035 - 5056

International Journal of
ELECTROCHEMICAL
SCIENCE
www.electrochemsci.org

Quantum Chemical Studies on the Corrosion Inhibition of Mild Steel by Some Triazoles and Benzimidazole Derivatives in Acidic Medium

Mwadham M Kabanda[1], *Lutendo C. Murulana*[1], *Muzaffer Ozcan*[2], *Faruk Karadag*[3], *Ilyas Dehri*[4], *I.B. Obot*[5], *Eno E. Ebenso*[1,*]

[1]Department of Chemistry, School of Mathematical and Physical Sciences, North-West University (Mafikeng Campus), Private Bag X2046, Mmabatho 2735, South Africa
[2] Department of Science and Technology Education, Faculty of Education, Cukurova University, 01330 Adana, Turkey
[3] Department of Physics, Cukurova University, 01330 Adana, Turkey
[4] Department of Chemistry, Korkutata University, 8000 Osmaniye, Turkey
[5] Department of Chemistry, University of Uyo, PMB 1017, Uyo, Nigeria
[*]E-mail: Eno.Ebenso@nwu.ac.za

Received: 18 April 2012 / *Accepted:* 29 April 2012 / *Published:* 1 June 2012

Quantum chemical calculations using the Density Functional Theory (DFT) method at three different basis sets, namely, 6-31(d,p), 6-31+(d,p) and 6-311G(d,p) were performed on selected triazole and benzimidazole derivatives, namely 2-aminobenzimidazole (ABI), 1,3-benzothiazole (BTH), benzotriazole (BTA), 2-methylbenzimidazole (MBI), 2-(2-pyridyl)benzimidazole (PBI), 2-(amino methyl)benzimidazole (AMBI), 5-amino-3-mercapto-1,2,4-triazole (5AMTZ), 2-hydroxybenzimidazole (HBI), benzimidazole (BI) and 5-amino-1,2,4-triazole (5ATZ), to determine their reactive centres which might interact with the metal surface on the adsorption of the these compounds onto the metal surface. The results show that the adsorption of the inhibitor onto the metal surface would preferentially be through the benzene ring that is fused to the heterocyclic ring and through the heteroatoms of the heterocyclic ring. The study on the protonated species of the studied compounds show that they have the least tendency to chemically adsorb onto the metal surface and might preferentially adsorb physically. The quantitative structure activity relationship approach indicates that three to four quantum chemical parameters are needed to effect a reasonable correlation between experimentally determined and theroetically estimated inhibition efficiencies.

Keywords: Triazole and benzimidazole derivatives; Corrosion inhibitors; DFT; molecular properties; QSAR approach.

1. INTRODUCTION

Several approaches have been suggested and implemented to protect metals from the effects of corrosion. Among these approaches is the use of corrosion inhibitors [1,2]. Corrosion inhibitors are substances that when adsorbed onto the metal-solution interface (through either physisorption or chemisorption) block the corrosive material (solution) from coming into contact with metal. Corrosion inhibitors are made from different types of substances, such as organic molecules, amino acid derivatives, ionic liquids, etc. The adsorption of the inhibitor on the metal surface is a complex mechanism involving a number of factors such as the nature of the metal, the environment, the electrochemical potential at the metal interface and nature of the inhibitor [3]. Therefore, to understand the whole mechanism, all the factors need to taken into consideration. The current work is concerned only with elucidating the influence of the nature of the inhibitor on its adsorption into the metal-solution interface. In the selection of a suitable compound for corrosion inhibition, the geometric and the electronic properties of the compound should also be taken into consideration as they influence the ability of the compound to cover the metal surface and the ability of the compound to react with the metal surface and therefore bind to the metal surface. Studies by other researchers have shown that compounds with planar geometry are preferred to compounds that have less planar geometry [4]. This is understood from the fact that a compound with planar geometry tends to have more of its atoms in contact with the metal surface than a compound that has less planar geometry, thus interactions with metal surfaces are more likely with a planar geometry than with a non-planar geometry.

Electronic properties (e.g., the electron density, the dipole moment, partial charges on the atoms, etc) of a molecule informs about its reactivity. The electronic properties are influenced by the type of the functional groups present in the molecule. Molecules that have functional groups with high electron density are preferred as corrosion inhibitors, mainly because the adsorption of the corrosion inhibitor on the metal surface requires that electrons are donated from the corrosion inhibitor to the partially filled or vacant d orbitals of the metal to form a coordinating bond between the inhibitor and the metal. Therefore molecules that have atoms with lone pair of electrons (e.g., heteroatoms such as N, O, S and P), π conjugate double bond and aromatic systems are preferred as corrosion inhibitors [5]. Studies in the area of electrochemistry have concluded that the order of inhibition efficiency preference by molecules containing heteroatoms is such that O < N < S < P [6]. This preference might be related to the electronegativity of the atoms involved. The O atom has the highest electronegativity and hence it has the lowest tendency to donate electrons to the metal while P has the lowest electronegativity value and therefore has the highest tendency to donate electrons to the metal.

Although the two factors influencing the selection of a suitable corrosion inhibitor have been discussed separately, they are inter-dependent of each other and therefore should be considered together to effect a proper selection of a good corrosion inhibitor. For instance, a molecule with less planar geometry but with more electron donor centres may be preferred to a molecule that is highly planar but with less electron donor centres. Several approaches are employed in elucidating the characteristics of compounds that have the potential to be effective corrosion inhibitors, among which is the use of quantum chemical calculation methods. These methods are able to estimate the geometry of molecules and to provide not only the electronic parameters, but also to inform about the reactivity

and selectivity of the molecules. In the last decade there has an increase, in the area of corrosion science, in the utilization of quantum chemical calculation methods to obtain molecular properties that might be helpful in selecting potential molecules, among a list of molecules, as possible candidates for corrosion inhibition. Most importantly, quantum chemical calculation methods are also extensively utilized to help explain trends in experimental results, for cases where such information would be rarely available from experimental data. In the current work, quantum chemical calculations have been used to explain the results of experimental work on selected triazole and benzimidazole derivatives in an attempt to understand their molecular properties influencing their role as corrosion inhibitors.

Several researchers have reported the role of some triazole and benzimidazole derivatives as corrosion inhibitors on different metal surfaces and in different environments [7−24]. Both experimental techniques [7−15] and theoretical quantum chemical calculation methods [16, 20−24] have been utilized in the study of some of these triazole and benzimidazole derivatives as corrosion inhibitors. All these studies have confirmed the potential role of triazole and benzotriazole derivatives as corrosion inhibitors. Some of the triazole and benzomidazole derivatives investigated in the current work include a number of those compounds previously studied by other groups; but however, the current work presents the largest set of triazole and benzimidazole derivatives studied up-to-date which makes it more interesting in terms of comparison across structures.

The objective of this work therefore is to investigate the structures and molecular properties of three (3) selected triazole derivatives and eight (8) benzimidazole derivatives using the Density Funtional Theory (DFT) method with three different basis sets. The molecular properties [e.g., the highest occupied molecular orbital (HOMO), the lowest unoccupied molecular orbital (LUMO), ionisation potential (IP), electron affinity (EA), electronegativity (χ), global hardness and global softness] obtained are then utilized to elucidate the reactive sites in the different structures and the reactivity trends among structures. Furthermore, trends in the calculated quantum chemical descriptors are compared with the trends in the corrosion inhibition efficiency of the compounds. Quantitative structure activity relationship (QSAR) approach is utilized to determine possible correlation between experimental inhibition efficiencies of the compounds and two or more quantum chemical parameters of the compounds.

2. COMPUTATIONAL APPROACH

Calculations were done by using the Density Functional Theory (DFT) method in combination with the B3LYP functional. The DFT/B3LYP combination is known to produce good estimate of molecular properties that are related to molecular reactivity [25]. Three basis sets, viz., 6-31G(d,p), 6-31+G(d,p) and the 6-311G(d,p) were utilized for the calculations. The use of the 6-31+G(d,p) was meant to investigate the influence of addition of diffuse orbitals on the calculated molecular parameters. Among the molecular properties that are well reproduced by DFT/B3LYP include the energy of the highest occupied molecular orbital (HOMO), energy of the lowest unoccupied molecular orbital (LUMO), electronegativity, global hardness and softness, electron affinity, ionisation potential, etc. These quantities are often defined following Koopmans' theorem [26, 27]. Electronegativity (χ) is

the measure of the power of an electron or group of atoms to attract electrons towards itself [28] and according to Koopman's theorem, it can be estimated by using the following equation:

$$\chi \cong -\frac{1}{2} (E_{HOMO} + E_{LUMO}) \quad (1)$$

where E_{HOMO} is the energies of the highest occupied molecular orbital (HOMO) and and E_{LUMO} is the energy of the lowest unoccupied molecular orbital (LUMO).

Global hardness (η) measures the resistance of an atom to a charge transfer [29] and it is estimated using the equation:

$$\eta \cong -\frac{1}{2} (E_{HOMO} - E_{LUMO}) \quad (2)$$

Global softness (σ) describes the capacity of an atom or group of atoms to receive electrons [29] and it is estimated by using the equation:

$$\sigma = 1/\eta \cong -2/(E_{HOMO} - E_{LUMO}) \quad (3)$$

where η is the global hardness values

Global electrophilicity index (ω) is estimated by using the electronegativity and chemical hardness parameters through the equation:

$$\omega = \chi^2/2\eta \quad (4)$$

A high value of electrophilicity describes a good electrophile while a small value of elecrophilicity describes a good nucleophile.

Electron affinity (EA) is related to E_{LUMO} through the equation:

$$EA \cong - E_{LUMO} \quad (5)$$

Ionization potential (IP) is related to the E_{HOMO} through the equation:

$$IP \cong - E_{HOMO} \quad (6)$$

The change in the number of electrons transferred is estimated through the equation

$$\Delta N = \chi_{Fe} - \chi_{inh} / 2(\eta_{Fe} - \eta_{inh}) \quad (7)$$

where χ_{Fe} and χ_{inh} denote the absolute electronegativity of iron and the inhibitor molecule respectively; η_{Fe} and η_{inh} denote the absolute hardness of iron and the inhibitor molecule respectively. The values of χ_{Fe} and η_{Fe} are taken as 7 $eVmol^{-1}$ and 0 $eVmol^{-1}$ respectively [30].Frequency calculations were performed on optimized geometries to establish the nature of the stationary point on

the potential energy surface. Calculation in solution were performed by utilizing the PCM model as implemented in the Gaussian03 package [31]. The quantitative structure activity relationship were performed using the xlstart program [32].

3. RESULTS AND DISCUSSIONS

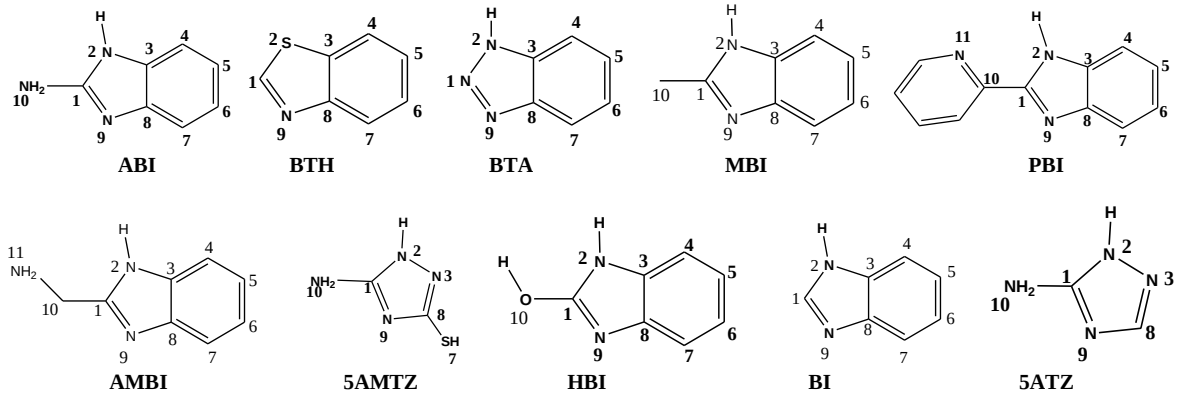

names of the compounds	acronym used
2-aminobenzimidazole	ABI
1,3-benzothiazole	BTH
benzotriazole	BTA
2-methylbenzimidazole	MBI
2-(2-pyridyl)benzimidazole	PBI
2-(amino methyl)benzimidazole	AMBI
5-amino-3-mercapto-1,2,4-triazole	5AMTZ
2-hydroxybenzimidazole	HBI
benzimidazole	BI
5-amino-1,2,4-triazole	5ATZ

Figure 1. The schematic representation of the structures of the studied compounds and the acronyms of the names of the compounds. Structures are arranged in order of decreasing inhibition efficiency of the inhibitors.

Table 1. Compounds used as inhibitors and the corresponding percent inhibition efficiencies obtained by using the weight loss method.

Compound	abbreviated name of the compound	%IE (30°C) [a]
2-aminobenzimidazole	ABI	96.5
1,3-benzothiazole	BTH	90.4
benzotriazole	BTA	89.4
2-methylbenzimidazole	MBI	85.4
2-(2-pyridyl)benzimidazole	PBI	71.2
2-(amino methyl)benzimidazole	AMBI	69.4
5-amino-3-mercapto-1,2,4-triazole	5AMTZ	60.2
2-hydroxybenzimidazol	HBI	60.1
benzimidazole	BI	58.4
5-amino-1,2,4-triazole	5ATZ	38.1

[a] The inhibition efficiency reported are those obtained at 30°C. The structures are arranged in order of decreasing inhibition efficiency

The selected triazole and benzimidazole derivatives are shown in figure 1 (together with the atom numbering utilized throughtout the this work) namely 2-aminobenzimidazole (ABI), 1,3-benzothiazole (BTH), benzotriazole (BTA), 2-methylbenzimidazole (MBI), 2-(2-pyridyl)benzimidazole (PBI), 2-(amino methyl)benzimidazole (AMBI), 5-amino-3-mercapto-1,2,4-triazole (5AMTZ), 2-hydroxybenzimidazole (HBI), benzimidazole (BI) and 5-amino-1,2,4-triazole (5ATZ).Throughout the discussion the structures will be referred to by their abbreviated names. The structures in figure 1 are arranged in order of decreasing experimentally determined inhibition efficiencies as reported in table 1. The experimentally determined inhibition efficiencies of the compounds,were obtained by using the gravimetric technique.

The results show that several quantum chemical parameters should be considered simultaneously in order to correlate the predicted inhibition efficiencies with the experimentally determined inhibition efficiencies. The results also show that preferred site for adsorption of triazole and benzomidazole derivatives is the N9 atom because it is the least sterically hindered heteroatom and has adequate negative partial charge.

3.1. The geometries and molecular properties of the non-protonated compounds

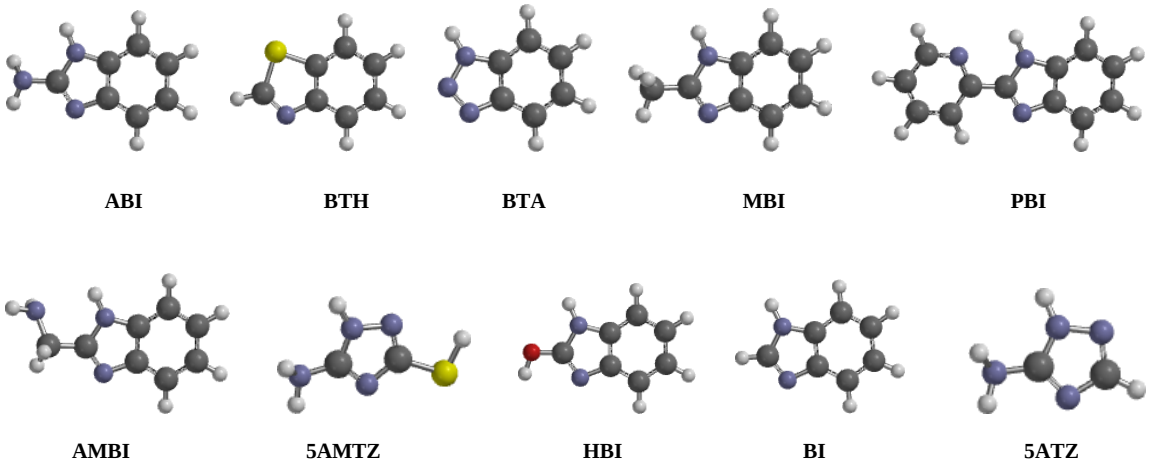

Figure 2. The optimised geometries of the studied compounds. The structures are arranged in order of decreasing inhbition efficiency (B3LYP/6-311G(d,p) results *in vacuo*).

Figure 2 reports the optimised structures of the studied molecules. The figure reports the lowest energy conformer corresponding to each structure. The geometries show that all the structures are highly planar with the exception of the hydrogen atoms of the methyl group in MBI and the amino group in AMBI. Table 2 shows the bond lengths of the different bond in the studied compounds; the C-S bond has the longest bond length and the smallest bond order (i.e., it is the weakest bond) while the N9-C1(N1) has the shortest bond length and largest bond order (i.e., it is the strongest bond in all the compounds).

Molecular properties of the studied compounds provide information on the reactivity and selectivity of the compounds; such information is useful in the comparison of the trends in reactivity

among different compounds and is important in the attempt to understand the interaction of the inhibitor with the metal surface.

Table 2. Comparison of the bond length (Å) in the non-protonated and the protonated species of the studies compounds.

bond	bond length (Å) for individual structures									
	ABI	BTH	BTA	MBI	PBI	AMBI	5AMTZ	HBI	BI	5ATZ
non-protonated										
1-2	1.380	1.768	1.363	1.382	1.374	1.374	1.352	1.368	1.377	1.355
	1.14	1.07	1.14	1.15	1.13	1.17	1.20	1.18	1.18	1.19
2-3	1.393	1.752	1.364	1.384	1.377	1.382	1.379	1.393	1.383	1.372
	1.03	1.12	1.04	1.06	1.09	1.07	1.07	1.03	1.06	1.10
3-4	1.389	1.396	1.400	1.393	1.395	1.394	1.316	1.389	1.395	
	1.36	1.35	1.29	1.34	1.33	1.34		1.36	1.33	
4-5	1.395	1.388	1.387	1.391	1.389	1.391		1.394	1.389	
	1.45	1.48	1.52	1.48	1.49	1.48		1.45	1.49	
5-6	1.402	1.404	1.414	1.406	1.409	1.407		1.403	1.408	
	1.41	1.38	1.35	1.39	1.37	1.39		1.41	1.38	
6-7	1.393	1.386	1.387	1.389	1.387	1.389		1.392	1.388	
	1.46	1.48	1.52	1.48	1.49	1.48		1.46	1.49	
7-8	1.395	1.401	1.401	1.397	1.400	1.398	1.769	1.394	1.399	
	1.38	1.36	1.31	1.37	1.35	1.36	1.03	1.38	1.35	
8-9	1.391	1.387	1.380	1.388	1.382	1.389	1.365	1.394	1.389	1.367
	1.31	1.25	1.33	1.32	1.35	1.33	1.33	1.30	1.33	1.36
9-1	1.306	1.287	1.286	1.308	1.315	1.308	1.321	1.299	1.304	1.320
	1.64	1.74	1.53	1.67	1.62	1.66	1.55	1.63	1.69	1.56
1-10	1.382			1.492	1.465	1.500	1.378	1.340		1.381
	1.09			1.01	1.10	0.99	1.10	1.16		1.09
10-11					1.344	1.471				
						1.02				
protonated										
1-2	1.346	1.696	1.308	1.340	1.338	1.330	1.334	1.334	1.333	1.340
	1.24	1.30	1.32	1.31	1.28	1.35	1.22	1.31	1.35	1.20
2-3	1.409	1.759	1.376	1.398	1.390	1.395	1.383	1.406	1.396	1.376
	1.00	1.15	1.03	1.04	1.07	1.05	1.07	1.00	1.04	1.09
3-4	1.387	1.395	1.399	1.392	1.393	1.392		1.388	1.394	
	1.38	1.35	1.29	1.34	1.34	1.34		1.36	1.33	
4-5	1.393	1.387	1.381	1.388	1.387	1.388		1.391	1.387	
	1.46	1.49	1.53	1.49	1.49	1.49		1.47	1.50	
5-6	1.401	1.407	1.418	1.407	1.408	1.407		1.403	1.410	
	1.42	1.37	1.33	1.38	1.38	1.38		1.41	1.37	
6-7	1.393	1.385	1.381	1.388	1.388	1.389		1.391	1.387	
	1.46	1.50	1.53	1.49	1.49	1.49		1.47	1.50	
7-8	1.387	1.396	1.399	1.392	1.392	1.392	1.748	1.388	1.394	
	1.38	1.34	1.29	1.34	1.34	1.34	1.14	1.36	1.33	
8-9	1.409	1.394	1.376	1.398	1.397	1.402	1.397	1.411	1.397	1.388
	1.00	1.01	1.03	1.04	1.06	1.04	1.09	0.99	1.04	1.11
9-1	1.346	1.322	1.308	1.340	1.345	1.340	1.355	1.340	1.333	1.354
	1.24	1.43	1.32	1.31	1.25	1.29	1.19	1.28	1.35	1.20
1-10	1.336			1.485	1.462	1.507	1.332	1.309		1.331
	1.24			1.03	1.12	0.95	1.25	1.29		1.26
10-11					1.343	1.459				
					1.43	1.05				

The selected molecular properties include the highest occupied molecular orbital (HOMO), the lowest unoccupied molecular orbital (LUMO), the energy of the HOMO (E_{HOMO}), the energy of the LUMO (E_{LUMO}), the energy difference between the HOMO and the LUMO (ΔE), the dipole moment,

molecular volume (MV), charges on the atoms, etc. The calculated molecular properties are reported in table 3.

Table 3. Quantum chemical descriptors for the studied compounds (Results with different calculation methods. Structures are arranged in order of decreasing inhibition efficiency as reported in table 1).

Structure	Quantum Chemical descriptor [a]												
	E_{HOMO}	E_{LUMO}	ΔE	IP	EA	χ	η	σ	ΔN	ω	μ	MV	pol
B3LYP/6-31G(d,p)													
ABI	–5.442	0.087	5.529	5.442	–0.087	2.678	2.765	0.362	0.782	1.297	3.81	136	51.07
BTH	–6.470	–1.018	5.452	6.470	1.018	3.744	2.726	0.367	0.597	2.571	1.21	132	50.77
BTA	–6.600	–1.213	5.387	6.600	1.213	3.907	2.694	0.371	0.574	2.833	3.98	117	49.62
MBI	–5.896	–0.239	5.657	5.896	0.239	3.068	2.829	0.354	0.695	1.663	3.50	144	51.69
PBI	–5.817	–1.454	4.363	5.817	1.454	3.636	2.182	0.458	0.771	3.029	2.53	203	56.80
AMBI	–5.791	–0.183	5.608	5.791	0.183	2.987	2.804	0.357	0.716	1.591	3.68	154	52.58
5AMTZ	–5.875	0.577	6.452	5.875	–0.577	2.649	3.226	0.310	0.674	1.088	4.38	94	47.48
HBI	–5.742	–0.017	5.725	5.742	0.017	2.880	2.863	0.349	0.720	1.448	2.24	132	50.74
BI	–6.079	–0.366	5.713	6.079	0.366	3.223	2.857	0.350	0.661	1.818	3.43	125	50.19
5ATZ	–6.197	0.707	6.904	6.197	–0.707	2.745	3.452	0.290	0.616	1.091	3.67	77	45.97
B3LYP/6-311G(d,p)													
ABI	–5.664	–0.181	5.483	5.664	0.181	2.923	2.742	0.365	0.744	1.558	3.94	135	51.06
BTH	–6.676	–1.246	5.430	6.676	1.246	3.961	2.715	0.368	0.56	2.889	1.24	131	50.75
BTA	–6.826	–1.450	5.376	6.826	1.450	4.138	2.688	0.372	0.532	3.185	3.99	117	49.60
MBI	–6.137	–0.514	5.623	6.137	0.514	3.326	2.812	0.356	0.653	1.967	3.56	143	51.68
PBI	–6.060	–1.709	4.351	6.060	1.709	3.885	2.176	0.460	0.716	3.468	2.59	203	56.78
AMBI	–6.025	–0.461	5.564	6.025	0.461	3.243	2.782	0.359	0.675	1.890	3.78	154	52.57
5AMTZ	–6.044	0.225	6.269	6.044	–0.225	2.910	3.135	0.319	0.652	1.350	4.44	94	47.51
HBI	–5.986	–0.298	5.688	5.986	0.298	3.142	2.844	0.352	0.678	1.736	2.29	132	50.74
BI	–6.317	–0.652	5.665	6.317	0.652	3.485	2.833	0.353	0.621	2.143	3.49	125	50.19
5ATZ	–6.385	0.350	6.735	6.385	–0.350	3.018	3.368	0.297	0.591	1.352	3.71	77	46.00
B3LYP/6-31+ G(d,p)													
ABI	–5.785	–0.508	5.277	5.785	0.508	3.147	2.639	0.379	0.73	1.876	3.90	136	51.14
BTH	–6.724	–1.363	5.361	6.724	1.363	4.044	2.681	0.373	0.551	3.050	1.40	132	50.80
BTA	–6.906	–1.596	5.310	6.906	1.596	4.251	2.655	0.377	0.518	3.403	4.21	117	49.64
MBI	–6.205	–0.643	5.562	6.205	0.643	3.424	2.781	0.360	0.643	2.108	3.66	144	51.72
PBI	–6.125	–1.815	4.310	6.125	1.815	3.970	2.155	0.464	0.703	3.657	2.56	203	56.83
AMBI	–6.124	–0.697	5.427	6.124	0.697	3.411	2.714	0.369	0.661	2.143	3.66	155	52.63
5AMTZ	–6.168	–0.627	5.541	6.168	0.627	3.398	2.771	0.361	0.65	2.083	4.37	94	47.70
HBI	–6.112	–0.497	5.615	6.112	0.497	3.305	2.808	0.356	0.658	1.945	2.23	132	50.78
BI	–6.397	–0.825	5.572	6.397	0.825	3.611	2.786	0.359	0.608	2.340	3.58	125	50.23
5ATZ	–6.573	–0.532	6.041	6.573	0.532	3.553	3.021	0.331	0.571	2.089	3.76	77	46.17

[a] MV is Molecular volume, IP is Ionization potential, EA is Electron affinity, ΔN is Fraction of electrons transferred

The highest occupied molecular orbital (HOMO) gives information about the regions in the molecule with the most energetic electrons. These electrons are the most likely to be donated to the electron poor species. Figure 3 shows the HOMO and the LUMO for the studied compounds. The

results shows that the HOMO is spread throughout much of the compound, therefore for better understanding of the HOMO, it is important to examine the coefficients of the HOMO. The coefficient of the HOMO which gives information about the atomic orbital with the highest contribution to the HOMO and therefore the atom (in a molecule) that has the highest tendency to donate electrons.

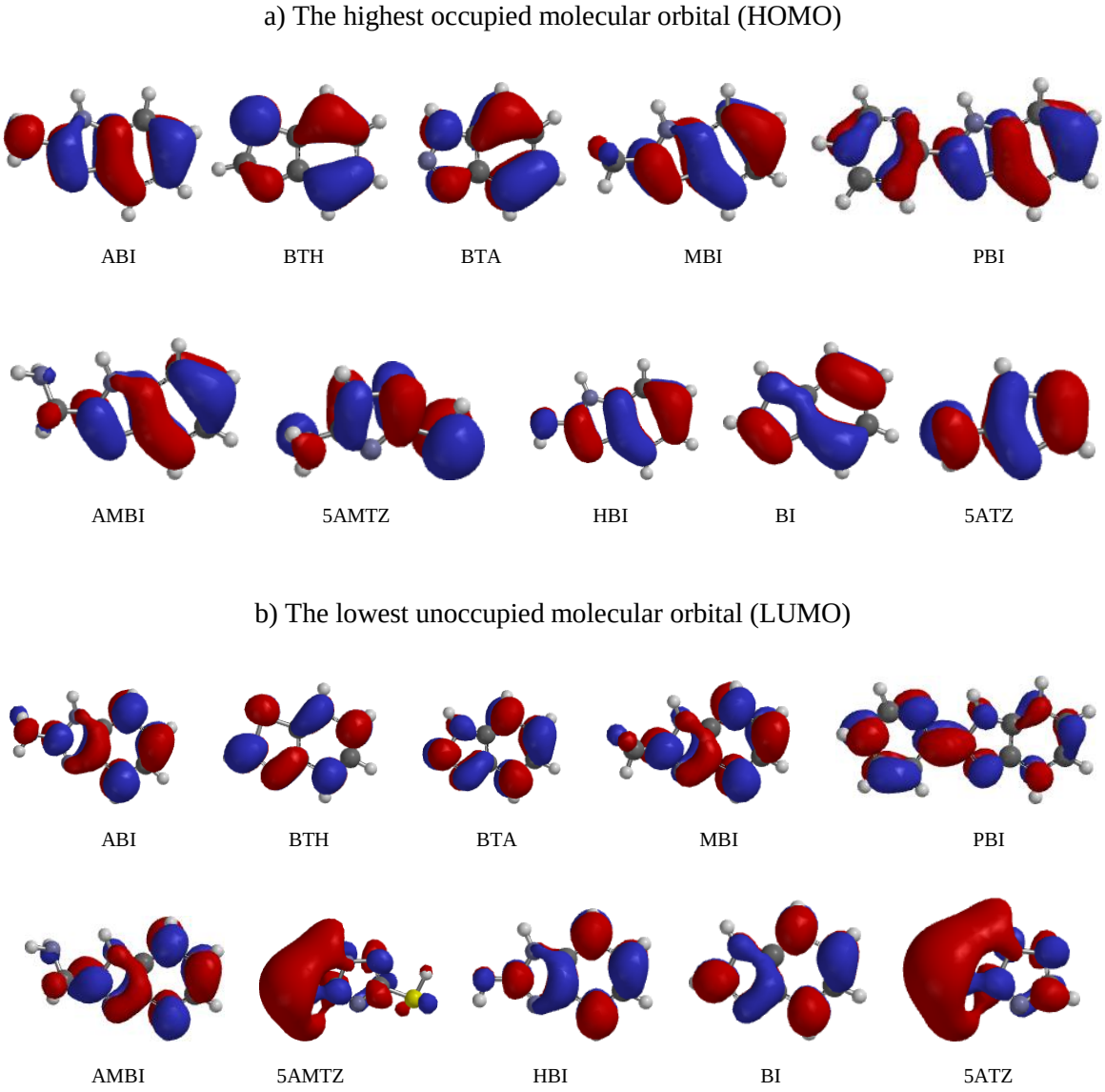

Figure 3. The highest Occupied molecular orbital and the lowest unoccupied molecular orbital for the studied compounds (B3LYP/6-311G(d,p) results).

The maximum coefficients of the HOMO for the different compounds are presented in table 4; eight out of the ten structures (ABI, BTH, BTA, MBI, PBI, AMBI, HBI and BI) have the highest coefficient of the HOMO in the aromatic ring that is fused to the heterocylic ring, which implies that the electron donor role in these molecules is largely due to their aromatic nature; whereas 5AMTZ and

5ATZ have the highest coefficient of the HOMO on the N3 atom. 5AMTZ and 5ATZ also have a high coefficient of the HOMO on S7 and N10 respectively.

Table 4. The highest coefficient of the HOMO and the LUMO of the studied molecule (B3LYP/6-311G(d,p) results).

Structure	Atom numbering [a] and the corresponding maximum coefficient of the HOMO and the LUMO										
	1	2	3	4	5	6	7	8	9	10	11
Coefficients of the HOMO											
ABI	0.10286	0.02338	–0.1085	0.0212	0.12381	0.06366	–0.0726	–0.1061	0.10600	–0.1100	
BTH	–0.0321	–0.1069	–0.0385	–0.1326	–0.0636	0.08653	0.12816	0.01495	–0.0934		
BTA	0.00494	–0.1287	0.05449	0.1372	0.04079	–0.1161	–0.1299	0.01576	0.09881		
MBI	0.12028	–0.0217	–0.0949	0.0627	0.13616	0.0437	–0.0913	–0.1130	0.09507	–0.0254	
PBI	0.11409	0.00353	–0.1028	0.0334	0.12288	0.05884	–0.0685	–0.1077	0.08504	–0.0023	–0.0468
AMBI	0.11492	–0.0302	–0.0899	0.0668	0.13357	0.03606	–0.0948	–0.1072	0.09889	–0.0266	0.01282
5AMTZ	0.07425	0.11191	–0.1558				–0.1259	–0.0925	0.00876	–0.0913	
HBI	0.1086	0.01552	–0.1102	0.0302	0.13134	0.06709	–0.0738	–0.1154	0.10040	–0.1011	
BI	–0.0934	0.08043	0.04382	–0.1138	–0.1202	0.02109	0.12675	0.07906	–0.1102		
5ATZ	–0.1057	–0.0917	0.16266					0.09603	–0.0958	0.15193	
Coefficients of the LUMO											
ABI	0.13173	–0.0337	–0.0457	0.1488	–0.1075	-0.0471	0.14983	–0.0927	–0.0377	–0.0458	
BTH	0.17552	0.06284	0.05448	0.0853	–0.1168	0.0019	0.1063	–0.0858	–0.1073		
BTA	0.16562	–0.0824	0.00357	0.1251	–0.1106	-0.0493	0.13579	–0.0547	–0.1039		
MBI	0.14568	–0.0563	–0.0235	0.1378	–0.1103	-0.0437	0.1429	–0.0816	–0.0670	0.00423	
PBI	0.08702	–0.0715	0.02592	0.0576	–0.0642	-0.0287	0.07112	–0.0125	–0.0954	0.00702	–0.1178
AMBI	0.13946	–0.0600	–0.0254	0.1329	–0.1019	-0.0477	0.13713	–0.0712	–0.0692	0.00969	–0.0011
5AMTZ	0.10732	–0.0821	0.09488				–0.0162	–0.0696	–0.0264	–0.0006	
HBI	0.12519	–0.0292	–0.0548	0.1551	–0.1056	-0.0543	0.15556	–0.0924	–0.0321	–0.0616	
BI	0.14447	–0.0635	–0.0241	0.1391	–0.1094	-0.0479	0.14411	–0.0766	–0.0743		
5ATZ	0.11193	–0.0886	0.10705					–0.0737	–0.0247	0.00244	

[a] The numbering 1,2,3… on separate columns represent the atom numbering for individual structures as shown in figure 1.

The LUMO is the unoccupied orbital that has the lowest energy and gives information on the regions in a molecule that have the highest tendency to accept electrons from an electron rich species. Figure 3 and table 4 also respectively shows the LUMO and the highest coefficient of the LUMO for the studied molecules; seven out of the 10 structures (BTH, BTA, MBI, AMBI, 5AMTZ, BI and 5ATZ) have the highest coefficient of the LUMO on position 1 of the heterocyclic ring (the numbering of the atoms is shown in figure 1). However, several molecules have a high coefficient of the LUMO also in the aromatic ring (C4 and C7 atoms), suggesting that the aromatic ring in these molecules might play a role in the back donation effect with the metal surface (i.e., for cases where the metal can donate its d orbital electrons to the inhibitors).

The energy of the HOMO (E_{HOMO}) provides information about the tendency of a molecule to donate electrons to an electron poor species. The higher the E_{HOMO} is, the greater is the tendency of a molecule to donate its electrons to the electron poor species. Therefore a comparison of the E_{HOMO} of the studied compounds provides an indication of the molecules that would have the highest tendency to donate electrons to the metal. The results shows that, with all the methods, ABI has the highest E_{HOMO} and 5ATZ has the lowest E_{HOMO}, which implies that ABI would have the highest tendency to donate its

electrons to the metal surface and therefore bind strongly on the metal surface, while 5ATZ would have the least tendency to donate its electrons to the metal surface and would have the minimal binding effect on the metal surface. These results are in good agreement with experimental results that show that ABI has the highest inhibition efficiency while 5ATZ has the lowest inhibition efficiency. However the overall trend in the E_{HOMO} across all the ten compound does not agree completely with the trend in the inhibition efficiencies of the compounds.

The energy of the LUMO (E_{LUMO}) provides information about the tendency of a molecule to accept electrons from an electron rich species. The lower E_{LUMO} is, the greater is the tendency of a molecule to accept electrons from an electron rich species. The trend in the E_{LUMO} energy (from B3LYP/6-31G(d,p) and B3LYP/6-311G(d,p) results) for the studied compounds shows that PBI has the lowest E_{LUMO} while 5ATZ has the highest E_{LUMO}. The B3LYP/6-31G(d,p) method predicts that on the the addition of diffuse orbitals (i..e, on using the B3LYP/6-31+G(d,p) method), PBI has the lowest E_{LUMO} while ABI has the highest E_{LUMO}. Trends in the E_{LUMO} (by either method) across all the compounds, do not agree with the trends in the experimentally determined inhibition efficiency.

The energy difference between the HOMO and the LUMO (ΔE) provides information about the overall reactivity of a molecule; the smaller the ΔE value is, the greater is the reactivity of a molecule [33]. The trends in the ΔE values for the studied compounds show that PBI is the most reactive compound while 5ATZ is the least reactive compound. Therefore on interaction with the metal surface, PBI would have the highest tendency to interact with the metal surface; PBI has the highest electron density (charge density) centres because of the presence of the pyridium ring at C1 that is capable of donating electrons. The overall trend in the ΔE value across compounds, however, does not correlate well with the trend in the experimental inhibition efficiencies of the inhibitors.

The dipole moment provides information on the polarity of the molecule and it is also a good reactivity indicator. In the study of corrosion inhibitors, the dipole moment, as reactivity indicator, does not show univocal trends with the inhibition efficiencies of the inhibitors. For instance, the dipole moment has been reported to increase with the increase in inhibition efficiency of the inhibitors [34]; the dipole moment has also been reported to decrease with the increase in the inhibition efficiency of the inhibitors [35] and still there are literature works that show that the dipole moment does not correlate well with the corrosion inhibition efficiencies of the inhibitors [5]. In the current work, the trend across structures in the dipole moment of the compounds is not in good agreement with the trend in the inhibition efficiencies of the inhibitors. Molecular volume (MV) indicates possible metal surface coverage by the inhibitor. The larger the molecular volume of an inhibitor is, the greater is the inhibition efficiency because large molecule volume implies increased surface coverage. A comparison of the molecular volume of the studied compounds shows that PBI has the largest molecular volume while 5ATZ has the smallest molecular volume which indicates that PBI would be the most preferred corrosion inhibitor while 5ATZ would be the least preferred. However, in spite of predicting 5ATZ as the least preferred corrosion inhibitor, the trend in the MV values does not correlate well with the experimentally determined inhibition efficiencies.

The number of electrons transferred (ΔN) indicates the tendency of a molecule to donate electrons. The higher the value of ΔN is, the greater the tendency of a molecule to donate electrons to the electron poor species. In the case of corrosion inhibitors, a higher ΔN implies a greater tendency to

interact with the metal surface (i.e., a greater tendency to adsorb on the metal surface). ABI has the highest ΔN value while BTA has the least ΔN value. However, the trend in the ΔN value across structures does not correlate well with the trend in the experimentally determined inhibition efficiency. Beside reactivity indicators, several molecular properties are good indicators of selectivity (i.e., the regions on the molecule on which certain type of reactions are likely to occur) and include the partial atomic charges and the condensed Fukui functions. The atom with the highest negative partial charge is considered a possible site for an attack by electron deficient species [36].

Table 5. The Mulliken atomic charges on the atoms of the studied molecule (B3LYP/6-31G(d,p) and B3LYP/6-311G(d,p) results).

Structure	Atom numbering [a] and the corresponding Mulliken atomic charge										
	1	2	3	4	5	6	7	8	9	10	11
B3LYP/6-31G(d,p)											
ABI	0.649	–0.644	0.314	–0.115	–0.109	–0.098	–0.132	0.226	–0.556	–0.659	
BTH	–0.060	0.217	–0.147	–0.113	–0.074	–0.104	–0.080	0.251	–0.418		
BTA	–0.038	–0.473	0.353	–0.092	–0.098	–0.103	–0.086	0.223	–0.357		
MBI	0.473	–0.639	0.320	–0.108	–0.106	–0.100	–0.120	0.208	–0.533	–0.390	
PBI	0.481	–0.659	0.336	–0.107	–0.104	–0.100	–0.120	0.219	–0.578	0.267	–0.540
AMBI	0.478	–0.624	0.320	–0.108	–0.107	–0.100	–0.122	0.207	–0.553	–0.126	–0.623
5AMTZ	0.671	–0.389	–0.298				0.036	0.224	–0.504	–0.655	
HBI	0.702	–0.639	0.318	–0.110	–0.108	–0.098	–0.127	0.220	–0.561	–0.540	
BI	0.282	–0.604	0.313	–0.103	–0.105	–0.100	–0.112	0.206	–0.498		
5ATZ	0.659	–0.382	–0.281					0.225	–0.500	–0.656	
B3LYP/6-311G(d,p)											
ABI	0.464	–0.467	0.178	–0.054	–0.116	–0.104	–0.072	0.008	–0.368	–0.484	
BTH	–0.086	0.231	–0.256	–0.067	–0.084	–0.104	–0.033	0.139	–0.283		
BTA	–0.007	–0.362	0.232	–0.040	–0.101	–0.104	–0.030	–0.008	–0.234		
MBI	0.245	–0.454	0.187	–0.053	–0.112	–0.105	–0.064	–0.012	–0.332	–0.282	
PBI	0.393	–0.454	0.197	–0.052	–0.110	–0.106	–0.064	–0.013	–0.356	0.037	–0.366
AMBI	0.256	–0.433	0.188	–0.054	–0.113	–0.106	–0.067	–0.020	–0.341	–0.092	–0.486
5AMTZ	0.477	–0.297	–0.214				0.028	0.084	–0.361	–0.483	
HBI	0.462	–0.452	0.183	–0.047	–0.114	–0.104	–0.062	–0.006	–0.378	–0.346	
BI	0.177	–0.423	0.178	–0.046	–0.110	–0.104	–0.053	–0.016	–0.316		
5ATZ	0.460	–0.295	–0.199					0.090	–0.362	–0.480	

[a] The numbering 1,2,3… on top of each separate columns represents the atom numbering for individual structures as shown in figure 1.

Table 5 reports the Mulliken atomic charges obtained with both B3LYP/6-31G(d,p) and B3LYP/6-311G(d,p) methods. The results show that the N atoms have the highest negative charge; the S atom, in BTH and 5AMTZ, is electron deficient; the benzene ring has a delocalisation of slightly negative charge on its atoms; the carbon atom at C1 (i.e., in all the structures except BTH and BTA) is the most electron deficient. These results suggest that the N atoms in all the structures and the O atom in HBI are possible sites for adsorption by the inhibitor on the metal surface. However, most N atoms are sterically hindered or are saturated (i.e., they have three single bonds) except the N9 atom in all the structures and N3 in 5ATZ, suggesting that these are the probable centres that might interact with the metal surface resulting in a formation of a chemical bond with the metal.

Table 6. The condensed Fukui functions on the atoms of the studied molecule (B3LYP/6-311G(d,p) results).

Structure	Atom numbering [a] and the corresponding condensed Fukui functions										
	1	2	3	4	5	6	7	8	9	10	11
					f^+ function						
ABI	–0.033	0.010	–0.010	–0.096	–0.046	–0.008	–0.099	–0.017	–0.032	0.006	
BTH	–0.116	–0.206	0.003	–0.048	–0.074	–0.005	–0.087	–0.010	–0.069		
BTA	–0.154	–0.022	–0.011	–0.112	–0.058	–0.014	–0.120	–0.010	–0.086		
MBI	–0.065	–0.008	–0.009	–0.107	–0.055	–0.008	–0.114	–0.013	–0.048	–0.007	
PBI	–0.048	–0.009	–0.012	–0.048	–0.032	–0.012	–0.057	0.003	–0.040	–0.056	–0.044
AMBI	–0.060	–0.002	–0.006	–0.091	–0.043	–0.011	–0.096	–0.006	–0.046	0.021	0.038
5AMTZ	0.048	0.059	–0.040				–0.221	0.006	–0.014	0.061	
HBI	–0.092	–0.002	–0.016	–0.129	–0.052	–0.011	–0.129	–0.022	–0.039	–0.051	
BI	–0.128	–0.001	–0.009	–0.117	–0.055	–0.011	–0.120	–0.010	–0.052		
5ATZ	0.075	0.066	–0.062					–0.050	–0.023	0.086	
					s^+ function						
ABI	–0.012	0.004	–0.004	–0.035	–0.017	–0.003	–0.036	–0.006	–0.012	0.002	
BTH	–0.043	–0.076	0.001	–0.018	–0.027	–0.002	–0.032	–0.004	–0.025		
BTA	–0.057	–0.008	–0.004	–0.042	–0.022	–0.005	–0.045	–0.004	–0.032		
MBI	–0.023	–0.003	–0.003	–0.038	–0.020	–0.003	–0.041	–0.005	–0.017	–0.003	
PBI	–0.022	–0.004	–0.006	–0.022	–0.015	–0.006	–0.026	0.001	–0.018	–0.026	–0.020
AMBI	–0.022	–0.001	–0.002	–0.033	–0.015	–0.004	–0.035	–0.002	–0.017	0.008	0.014
5AMTZ	0.015	0.019	–0.013				–0.071	0.002	–0.005	0.020	
HBI	–0.032	–0.001	–0.006	–0.045	–0.018	–0.004	–0.045	–0.008	–0.014	–0.018	
BI	–0.045	0.000	–0.003	–0.041	–0.019	–0.004	–0.042	–0.004	–0.018		
5ATZ	0.022	0.020	–0.018					–0.015	–0.007	0.026	
					f^- function						
ABI	–0.077	–0.009	–0.059	–0.051	–0.078	–0.033	–0.065	–0.028	–0.076	–0.094	
BTH	–0.027	–0.267	0.024	–0.101	–0.037	–0.050	–0.110	–0.003	–0.072		
BTA	–0.081	–0.074	–0.010	–0.132	–0.026	–0.074	–0.118	–0.010	–0.091		
MBI	–0.071	–0.011	–0.049	–0.067	–0.089	–0.027	–0.076	–0.035	–0.069	–0.015	
PBI	–0.070	–0.005	–0.048	–0.044	–0.068	–0.029	–0.053	–0.027	–0.045	–0.013	–0.011
AMBI	–0.074	–0.010	–0.049	–0.064	–0.086	–0.026	–0.074	–0.032	–0.068	–0.010	–0.013
5AMTZ	–0.059	–0.050	–0.152				–0.359	–0.006	–0.060	–0.088	
HBI	–0.086	–0.010	–0.061	–0.057	–0.087	–0.036	–0.067	–0.037	–0.078	–0.093	
BI	–0.074	–0.039	–0.070	–0.080	–0.033	–0.106	–0.063	–0.036	–0.054		
5ATZ	–0.089	–0.041	–0.185					–0.190	–0.106	–0.160	
					s^- function						
ABI	–0.028	–0.003	–0.022	–0.019	–0.029	–0.012	–0.024	–0.010	–0.028	–0.034	
BTH	–0.010	–0.098	0.009	–0.037	–0.014	–0.018	–0.041	–0.001	–0.027		
BTA	–0.030	–0.028	–0.004	–0.049	–0.010	–0.028	–0.044	–0.004	–0.034		
MBI	–0.025	–0.004	–0.017	–0.024	–0.032	–0.010	–0.027	–0.013	–0.025	–0.005	
PBI	–0.032	–0.002	–0.022	–0.020	–0.031	–0.013	–0.024	–0.012	–0.021	–0.006	–0.005
AMBI	–0.027	–0.004	–0.018	–0.023	–0.031	–0.009	–0.027	–0.012	–0.024	–0.004	–0.005
5AMTZ	–0.019	–0.016	–0.049				–0.115	–0.002	–0.020	–0.028	
HBI	–0.030	–0.004	–0.022	–0.020	–0.031	–0.013	–0.024	–0.013	–0.028	–0.033	
BI	–0.026	–0.014	–0.025	–0.028	–0.012	–0.037	–0.022	–0.013	–0.019		
5ATZ	–0.026	–0.012	–0.055					–0.056	–0.032	–0.048	

[a] The numbering 1,2,3… on separate columns represent the atom numbering for individual structures as shown in figure 1.

The condensed Fukui functions are local selectivity descriptors. These functions inform about the centers in a molecule on which nucleophilic, electrophilic and radical reactions are most likely to occur. The Fukui functions for the electron rich centers (i.e., atoms susceptible to electrophilic attack)

and electron deficient centers (i.e., atoms that are susceptible to nucleophilic attack) are often estimated using the finite difference approximation approach [37]

$$f^{+} = q_{(N+1)} - q_N \qquad \text{for nucleophilic attack} \qquad (8)$$

$$f^{-} = q_N - q_{(N-1)} \qquad \text{for electrophilic attack} \qquad (9)$$

where $q_{(N+1)}$, q and $q_{(N-1)}$ are the charges of the atoms on the systems with N+1, N and N–1 electrons respectively. The preferred site for nucleophilic attack is the atom (or region) in the molecule where f^{+} has the highest value while the site for electrophilic attack is the atom (or region) in the molecule where the value of f^{-} is the highest. The estimated condensed Fukui functions for the non-hydrogen atoms, in the studied compounds, are reported in table 6. The preferred site for nucleophilic attack is position 1 of the heterocylic ring fused to the benzene ring; the C4 atom and the C7 atom. These results agree well with the analysis of the LUMO densities which also predicted these sites as the most electron deficient centers. The electrophilic attack (shown by the highest value of f^{-}) would preferably occur at C5 in ABI, MBI, PBI, AMBI and HBI; at C4 and C7 in BTA; at N3 in 5AMTZ and 5ATZ; at C6 in BI. The results also show that back donation might take place on the S atom in both BTH and 5AMTZ structures.

The local softness is defined as the product of the Fukui function and the global softness, σ and can be expressed as follows [38];

$$s^{+} = (f^{+})\sigma \qquad (10)$$

$$s^{-} = (f^{-})\sigma \qquad (11)$$

A high value of s^{+} indicates high nucleophilicity and a high value of s^{-} high electrophilicity. The results, reported in table 6, show that the trend in the s^{+} and s^{-} is similar to the trend in the f^{+} and f^{-} values.

3.2. Results of the study on the protonated species

In acidic environment the inhibitors also interact with the acidic solution leading to the possibility of co-existence of both protonated and non-protonated species of the inhibitor. In such cases, it is interesting to investigate the preferred species to interact with the metal surface and to study the influence of protonation on the molecular structures and the molecular properties of the inhibitors. The possible sites for protonation are the heteroatoms present in each compound. The results of the calculation on the different possible sites for protonation show that the preferred site for protonation is N9. This is the site that is less sterically hindered because there are no other protons present. Moreover, it is the only position that is common to all the selected compounds, making it easy to compare the effects of protonation across structures.

Figure 4 shows the optimized geometries of the protonated species together with the corresponding HOMO and LUMO. The bond lengths are reported in table 2, where they are compared with the corresponding bond lenghts of the non-protonated species. The results show that the C8–N9 and N9–C1(N1) bonds are longer in the protonated than in the non-protonated species; the corresponding bond orders are weaker in the protonated than in the non-protonated species. In the protonated species, the electron density of the C8–N9 bond and N9–C1(N1) bonds is less than that in the non-protonated species because of the need to stabilize the added proton at the N9 atom, consequently the two bonds are longer in the protonated than in the non-protonated species.

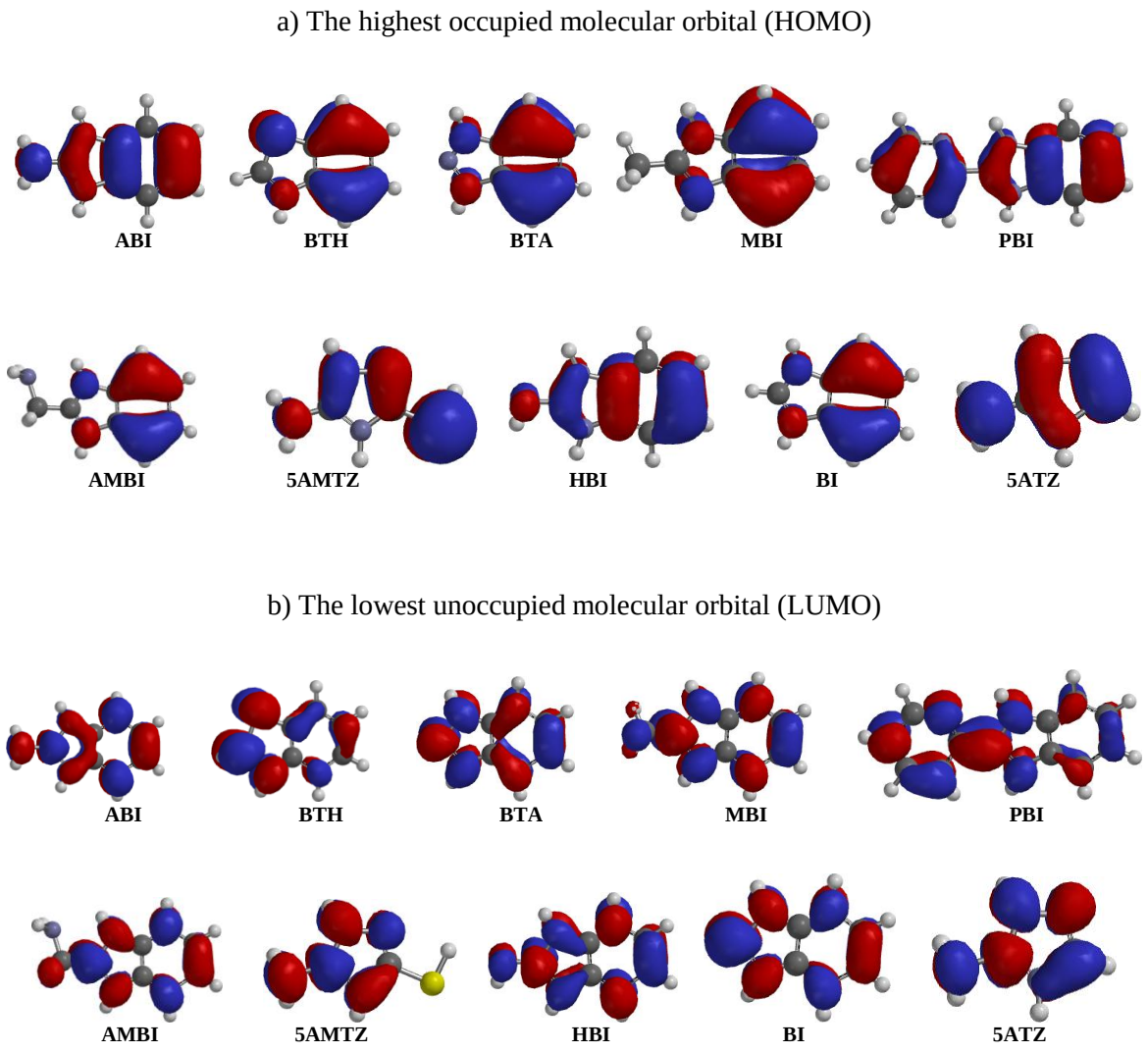

Figure 4. The highest Occupied molecular orbital and the lowest unoccupied molecular orbital for the protonated species of each of the studied compounds (B3LYP/6-311G(d,p) results).

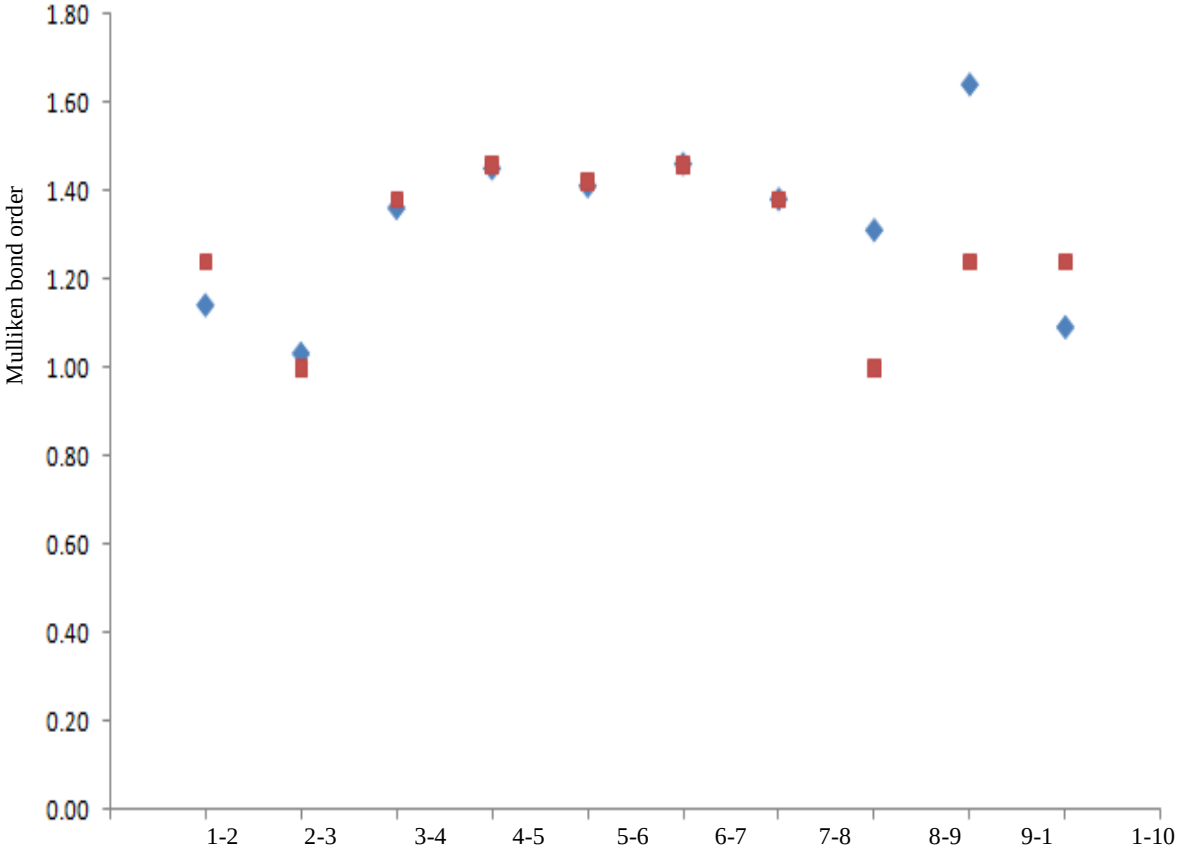

Figure 5. Comparison of the bond order in the non-protonated (◆) and the protonated (■) species of structure ABI. (B3LYP/6-311G(d,p) results. The trends in the bond order for other structures follows similar pattern. The numbering on the x axis refers to the atom numbering in figure 1).

A small bond order in the protonated species also suggests increased anti-bonding character related to the decrease in the electron density of each bond. Moreover, because of the rigidity of the heterocylic ring fused to the aromatic ring, the increase in the C8–N9 and N9–C1(N1) bond lengths also implies a decrease in the 1-2 and 7-8 bond lengths in the protonated species. The bond lengths in the benzene ring are slightly longer in the protonated than in the non-protonated species, indicating that there is minimal effects in the geometry of the aromatic ring as a result of protonation. Figure 5 shows the comparison of the bond order between the protonated and the non-protonated forms of ABI; the largest changes in the bond order involves the C8–N9 and N9–C1(N1); the bond order in the benzene ring shows minimal influence due to protonation.

The quantum chemical descriptors, such as the E_{HOMO}, E_{LUMO}, electronegativity, dipole moment, etc., are reported in table 7. The E_{HOMO} is lower in the protonated species than in the non-protonated species (by 4.423–5.848 eV), an indication that protonation decreases the electron donating ability of the inhibitors; E_{LUMO} is lower in the protonated species than in the non-protonated species (by 4.423–5.595), an indication of the increased electron accepting tendency of the inhibitors.

Table 7. Quantum chemical descriptors for the non-protonated and protonated studied compounds calculated at B3LYP/6-311G(d,p). Structures are arranged in order of decreasing inhibition efficiency as reported in table 1.

Structre	Quantum chemical descriptors [a]											
	E_{HOMO}	E_{LUMO}	ΔE	μ	MV	IP	EA	χ	η	σ	ΔN	ω
non-protonated												
ABI	–5.664	–0.181	5.483	3.94	135	5.664	0.181	2.923	2.742	0.365	0.744	1.558
BTH	–6.676	–1.246	5.430	1.24	131	6.676	1.246	3.961	2.715	0.368	0.560	2.889
BTA	–6.826	–1.450	5.376	3.99	117	6.826	1.450	4.138	2.688	0.372	0.532	3.185
MBI	–6.137	–0.514	5.623	3.56	143	6.137	0.514	3.326	2.812	0.356	0.653	1.967
PBI	–6.060	–1.709	4.351	2.59	203	6.060	1.709	3.885	2.176	0.460	0.716	3.468
AMBI	–6.025	–0.461	5.564	3.78	154	6.025	0.461	3.243	2.782	0.359	0.675	1.890
5AMTZ	–6.044	0.225	6.269	4.44	94	6.044	–0.225	2.910	3.135	0.319	0.652	1.350
HBI	–5.986	–0.298	5.688	2.29	132	5.986	0.298	3.142	2.844	0.352	0.678	1.736
BI	–6.317	–0.652	5.665	3.49	125	6.317	0.652	3.485	2.833	0.353	0.621	2.143
5ATZ	–6.385	0.350	6.735	3.71	77	6.385	–0.350	3.018	3.368	0.297	0.591	1.352
protonated												
ABI	–10.443	–4.748	5.695	6.73	138	10.443	4.748	7.596	2.848	0.351	-0.105	10.130
BTH	–11.437	–6.818	4.619	4.95	134	11.437	6.818	9.128	2.310	0.433	-0.461	18.037
BTA	–11.841	–7.045	4.796	2.68	119	11.841	7.045	9.443	2.398	0.417	-0.509	18.593
MBI	–11.009	–5.589	5.420	3.70	146	11.009	5.589	8.299	2.710	0.369	-0.240	12.707
PBI	–10.483	–6.141	4.342	1.48	205	10.483	6.141	8.312	2.171	0.461	-0.302	15.912
AMBI	–10.798	–5.305	5.493	3.96	157	10.798	5.305	8.052	2.747	0.364	-0.191	11.802
5AMTZ	–11.037	–4.741	6.296	3.28	97	11.037	4.741	7.889	3.148	0.318	-0.141	9.885
HBI	–10.938	–5.213	5.725	5.69	135	10.938	5.213	8.076	2.863	0.349	-0.188	11.391
BI	–11.261	–5.998	5.263	5.30	128	11.261	5.998	8.630	2.632	0.380	-0.310	14.149
5ATZ	–12.233	–4.959	7.274	3.27	79	12.233	4.959	8.596	3.637	0.275	-0.219	10.158

[a] MV is Molecular volume, IP is Ionization potential, EA is Electron affinity, ΔN is Fraction of electrons transferred

The molecular volume is higher for the protonated species than for the non-protonated species (by 2–3 A^3); ΔN value is higher for the non-protonated species than for the protonated species, a further indication of the preference of non-protonated species to donate electrons; the nucleophilicity index, ω, is higher for the protonated species than for the non-protonated species, an indication of the electron deficient nature of the protonated species. Collectively, the various molecular properties show that the protonated species have the least tendency to chemically adsorb on the metal surface. The interaction between the protonated and the metal surface might therefore involve physisoptiom mechanism, where the protonated species are attracted (through electrostatic interactions) to the metal surface by the already adsorbed anion [39].

The Mulliken atomic charges on the atoms of the protonated species are reported in table 8 and are compared with the corresponding Mulliken atomic charges on the non-protonated species. In comparison to the non-protonated species, all the atoms of the protonated species, with the exception of the N3/S3 and N9 atoms, are highly negative charge deficient, which indicates the minimal tendency for protonated species to chemically adsorb on the metal surface.

Table 8. Comparison of the Mulliken atomic charges in the non-protonated and the protonated species of the studies compounds.

Atom number	Mulliken atomic charges for individual structures									
	ABI	BTH	BTA	MBI	PBI	AMBI	5AMTZ	HBI	BI	5ATZ
non-protonated										
1	0.464	–0.086	–0.007	0.245	0.393	0.256	0.477	0.462	0.177	0.460
2	–0.467	0.231	–0.362	–0.454	–0.454	–0.433	–0.297	–0.452	–0.423	–0.295
3	0.178	–0.256	0.232	0.187	0.197	0.188	–0.214	0.183	0.178	–0.199
4	–0.054	–0.067	–0.040	–0.053	–0.052	–0.054		–0.047	–0.046	
5	–0.116	–0.084	–0.101	–0.112	–0.110	–0.113		–0.114	–0.110	
6	–0.104	–0.104	–0.104	–0.105	–0.106	–0.106		–0.104	–0.104	
7	–0.072	–0.033	–0.030	–0.064	–0.064	–0.067	0.028	–0.062	–0.053	
8	0.008	0.139	–0.008	–0.012	–0.013	–0.020	0.084	–0.006	–0.016	0.090
9	–0.368	–0.283	–0.234	–0.332	–0.356	–0.341	–0.361	–0.378	–0.316	–0.362
10	–0.484			–0.282	0.037	–0.092	–0.483	–0.346		–0.480
11					–0.366	–0.486				
protonated										
1	0.697	–0.004	0.107	0.343	0.512	0.386	0.712	0.581	0.304	0.707
2	–0.471	0.472	–0.291	–0.413	–0.419	–0.387	–0.303	–0.419	–0.381	–0.301
3	0.142	–0.340	0.179	0.135	0.147	0.143	–0.153	0.148	0.132	–0.119
4	–0.014	–0.039	0.015	–0.010	–0.015	–0.013		–0.004	0.001	
5	–0.086	–0.051	–0.073	–0.082	–0.082	–0.083		–0.082	–0.079	
6	–0.086	–0.085	–0.073	–0.082	–0.085	–0.085		–0.084	–0.079	
7	–0.014	0.004	0.014	–0.010	–0.017	–0.013	0.177	–0.004	0.001	0.230
8	0.142	0.314	0.178	0.135	0.127	0.126	0.161	0.132	0.132	–0.405
9	–0.470	–0.362	–0.290	–0.412	–0.458	–0.429	–0.417	–0.440	–0.380	–0.471
10	–0.477			–0.250	0.078	–0.095	–0.477	–0.262		
11					–0.373	–0.503				
variations [a]										
1	0.233	0.082	0.114	0.098	0.119	0.130	0.235	0.119	0.127	0.247
2	–0.004	0.241	0.071	0.041	0.035	0.046	–0.006	0.033	0.042	–0.006
3	–0.036	–0.084	–0.053	–0.052	–0.05	–0.045	0.061	–0.035	–0.046	0.080
4	0.040	0.028	0.055	0.043	0.037	0.041		0.043	0.047	
5	0.030	0.033	0.028	0.030	0.028	0.030		0.032	0.031	
6	0.018	0.019	0.031	0.023	0.021	0.021		0.020	0.025	
7	0.058	0.037	0.044	0.054	0.047	0.054	0.149	0.058	0.054	0.230
8	0.134	0.175	0.186	0.147	0.140	0.146	0.077	0.138	0.148	–0.495
9	–0.102	–0.079	–0.056	–0.080	–0.102	–0.088	–0.056	–0.062	–0.064	–0.109
10	0.007			0.032	0.041	–0.003	0.006	0.084		
11					–0.007	–0.017	0.235			

[a] The variations were calculated as ‘charges on the atom of the non-protonated species minus charge on the corresponding atom of the protonated species.

3.3. Quantitative structure activity relationships

The trends across structures in the individual quantum chemical properties discussed so far do not entirely agree with the trends in the experimentally determined inhibition efficiencies of the inhibitors. This is not surprising considering that there might be multiple inter-related factors contributing to the effectiveness of the studied compounds as corrosion inhibitors. On this account it is suitable to form a composite of several quantum chemical descriptors and attempt to correlate the composite index of these quantum chemical parameters to the experimentally determined inhibition efficiencies. This technique in which more than one quantum chemical parameters are correlated to the observed activity of the molecule is known as quantitative structure activity relationship. In this approach, a relationship in the form of an equation is sought which correlates the quantum chemical parameters to the observed activity. The linear and the non-linear equations, proposed by Lukovits, are

often used in the study of corrosion inhibitors to correlate the quantum chemical parameters with the experimental inhibition efficiency of the inhibitors [40, 41]. Only the linear equation has been found to provide good correlation for the quantum chemical parameters of triazole and benzimidazole derivatives. This equation has the form

$$IE_{theor} = Ax_i C_i + B \quad (11)$$

where A and B are the regression coefficients determined through regression analysis, x_i is a quantum chemical index characteristic of the molecule i, C_i is the experimental concentration of the inhibitor. The R^2 correlation value is in the range of 0.714–0.761 when using three to four molecular parameters derived from B3LYP/6-311+G(d,p) results. The best equation (corresponding to R^2 = 0.761, SSE = 729 and RMSE = 11) has the form

$$IE = -410.171*E_{LUMO} - 5831.573*\sigma + 2170.484*\Delta N + 507.239 \quad (12)$$

where E_{LUMO} is the energy of the LUMO, σ is the global softness and ΔN is the amount of electrons transferred. The equation therefore gives information that the best estimation of inhibition efficiency is obtained for decreasing values of E_{LUMO}, decreasing values of σ and increasing values of ΔN.

Table 9. Quantum chemical parameters utilised to form a composite index that was used to correlate quantum chemical parameters to experimentally determined inhibition efficiencies of the compounds. The quantum chemical parameters were obtained from B3LYP/6-31+G(d,p) results. QSAR derived equations and the corresponding R^2, SSE, MSE and RMSE values are also reported

Quantum chemical Parameters	Equation derived using the linear regression approach in [40]	R^2	SSE	RMSE
E_{LUMO},σ,ΔN	IE = -410.171*E_{LUMO}–5831.573*σ+ 2170.484*ΔN + 507.239	0.761	729	11
η,σ,ΔN and ω	IE = –499.973*η–7063.448*σ+1566.001*ΔN+214.936*ω+2539.948	0.758	736	12
η,σ,ΔN and E_{LUMO}	IE = –214.293*h–4991.119*s+1372.795*ΔN–261.342*E_{LUMO}+1410.127	0.749	765	12
χ,η,σ and ΔN	IE = 45.303*χ–560.495*η–3704.527*σ+214.382*ΔN+2668.614	0.720	852	13
χ,η,σ and MV	IE = 6.772*χ+-561.510*η+-3443.620*σ+7.396x10^{-2}*MV+2838.543	0.718	857	13
χ,η,σ and μ	IE = 5.101*χ–576.060*η–3469.231*σ–0.305*μ+2904.178	0.714	869	13

R^2 is the coefficient of determination, and *SSE* and RMSE are defined as

$$SSE = \sqrt{\sum_{i=1}^{n}\left(IE_{pred} - IE_{exp}\right)^2}$$

$$RMSE = \sqrt{\frac{1}{n}\sum_{j=1}^{n}\left(IE_{pred} - IE_{exp}\right)^2}$$

where IE_{pred} is the predicted inhibition efficiency and IE_{exp} is the experimental determined inhibition efficiency, n is the number of observations (compounds) considered

The combination of other quantum chemical parameters, the derived equations and the corresponding R^2, SSE and RMSE values are reported in table 9. Although the SSE values (i.e., sum of the squares of the error) are substantially large, the RMSE (i.e., the average error of the predicted value to the actual value) are reasonable small to suggest good correlation.

4. CONCLUSIONS

The following conclusions can be drawn from this study:

(a) Quantum chemical calculations, using the Density Functional Theory method, have been performed on triazole and benzimidazole derivatives to investigate their geometric and electronic properties in an attempt to elucidate the reactivity and selectivity centres of the compounds. The analysis of the HOMO, LUMO, partial atomic charges and the condensed fukui functions suggests similar centers that would be preferred for nucleophilic or electrophilic attack; the nucleophilic attack would preferentially occur on the position 1 at the heterocyclic ring fused to the benzene ring; the electrophilic attack would preferably occur on the benzene ring and on the N atoms of the heterocyclic ring fused to the benzene ring. Protonation has an influence on the molecular properties (e.g., E_{HOMO} and the E_{LUMO}) of the inhibitors. The results show that the protonated species have less charge density and therefore are less electron donor than the non-protonated species. Hence, in the interaction with the metal surface, the protonated species are most likely to interact with the metal surface through physisorption mechanism while the non-protonated species would preferentially interact with the metal surface through chemisorption mechanism.

(b) Quantitative structure activity relationships approach was used to correlate quantum chemical parameters with the experimentally determined inhibition efficiency. The results indicate that three to four quantum chemical parameters are required to form a composite index that on correlating with experimental determined inhibition efficiency gave good correlation (R^2 is in the range of 0.714–0.761).

(c) The study has therefore provided information that could be used to understand the factors contributing to the effectiveness of triazole and benzimidazole as corrosion inhibitors and used to select triazole and benzimidazole derivatives that are good corrosion inhibitors and also to design better corrosion inhibitors.

ACKNOWLEDGEMENTS

M. M. Kabanda is grateful to the North-West University for granting him a Postdoctoral Fellowship. E. E. Ebenso acknowledges the National Research Foundation (NRF) of South Africa for funding.

References

1. E-S. H. El Ashry, A. E-Nemr, S. A. Essawy, S. Ragab, *ARKIVOC* 2006 (xi) 205.
2. P. C. Okafor, E. E. Ebenso, U. J. Ekpe, *Int. J. Electrochem. Sci.* 5 (2010) 978.
3. F. Bentiss, B. Mernari, M. Traisnel, H. Vezin, M. Lagrenée. *Corros. Sci*. 53 (2011) 487.
4. F. Bentiss, M. Lagrenée, *J. Mater. Environ. Sci*. 2 (2011) 13.

5. N. O. Obi-Egbedi, I. B. Obot., M. I. El-Khaiary, S. A. Umoren, E. E. Ebenso. *Int. J. Electrochem. Sci.* 6 (2011) 5649.
6. J.G.N. Thomas, in: Proceedings of the Fifth European Symposium on Corrosion Inhibitors, Ann. Univ. Ferrara., Italy, 1980–1981, p. 453.
7. S.V. Lokesh, A. K. Satpati, B. S. Sherigara, *The Open Electrochem. J*. 2 (2010) 15.
8. R. Walker. Benzotriazole a corrosion inhibitor for antiques some practical surface chemistry. *J. Chem. Educ.*, 57 (1980) 789.
9. A.K. Satpati, P. V. Ravindran, *Mat. Chem. Phys*. 109 (2008) 352.
10. A.K. Satpati, M. M. Palrecha, R. I. Sundaresan, *Ind. J. Chem. Tech*. 15 (2008) 167.
11. A.K. Satpati, A. V. R. Reddy. Int. J. Electrochem. volume2011,Article ID173462, 8 pages.
12. A.Frignani, L. Tommesani, G. Brunoro, C. Monticelli, M. Fogagnolo, *Corros. Sci.* 41 (1999) 1205.
13. B. Sathianandhan, K. Balakrishnan, N. Subramanyan, *Br. Corros. J.* 43 (1987) 149.
14. F. Bentiss, M. Traisnel, H. Vezin, M. Lagrene´e, *Ind. Eng. Chem. Res*. 39 (2000) 3732.
15. F. Bentiss, M. Bouanis, B. Mernari, M. Traisnel, H. Vezin, M. Lagren´ee, *Appl. Surf. Sci*. 253 (2007) 3696.
16. W. Li, Q. He, C. Pei, B. Hou, *Electrochim. Acta* 52 (2007) 6386.
17. L. Wang, *Corros. Sci.*,48 (2006) 608.
18. T. Kosec, I. Miloˇsev, B. Pihlar, *Appl. Surf. Sci*. 253 (2007) 8863.
19. L. J. Berchmans, V.Sivan., S. V. K. Iyer, *Mater. Chem. Phys*. 98 (2006) 395.
20. K.F. Khaled, *Electrochim. Acta* 53 (2008) 3484.
21. K. F. Khaled, S. A. Fadl-Allah, B. Hammouti, *Mater. Chem. Phys*. 117 (2009) 148.
22. B. D. Mert, M. E. Mert, G. Kardaş, B. Yazıc. *Corros. Sci*. 53 (2011) 4265.
23. A.Y. Musa, A. A. H. Kadhum, A. B. Mohamad, M. S. Takriff. *Corros. Sci*. 52 (2010) 3331.
24. M. Finšgar, A. Lesar, A. Kokalj, Ingrid Milošev, *Electrochim. Acta* 53 (2008) 8287.
25. P. Senet, Chem. Phys. Lett. 275 (1997) 527.
26. P. Geerlings, F. De Proft, W. Langenaeker, *Chem. Rev*. 103 (2003) 1793.
27. R.G. Parr, R.G. Pearson, *J. Am. Chem. Soc*. 105 (1983) 7512.
28. L. Pauling, The Nature of the Chemical Bond (Coruell University Press, Ithaca, New York, 1960).
29. R.G. Parr, R.G. Pearson, *J. Am. Chem. Soc*. 105 (1983) 7512.
30. A.Y. Musa, A.A.H. Kadhum, A. B. Mohamed, M. S. Takriff, *Mater. Chem. Phys*. 129 (2011) 660.
31. Frisch, M. J.; Trucks, G. W.; Schlegel, H. B.; Scuseria, G. E.; Robb, M. A.; Cheeseman, J. R.; Montgomery, J. A.; Vreven, T.; Kudin, K. N.; Burant, J. C.; Millam, J. M.; Iyengar, S. S.; Tomasi, J.; Barone, V.; Mennucci, B.; Cossi, M.; Scalmani, G.; Rega, N.; Petersson, G. A.; Nakatsuji, H.; Hada, M.; Ehara, M.; Toyota, K.; Fukuda, R.; Hasegawa, J.; Ishida, M.; Nakajima, T.; Honda, Y.; Kitao, O.; Nakai, H.; Klene, M.; Li, X.; Knox, J. E.; Hratchian, H. P.; Cross, J. B.; Adamo, C.; Jaramillo, J.; Gomperts, R.; Stratmann, R. E.; Yazyev, O.; Austin, A. J.; Cammi, R.; Pomelli, C.; Ochterski, J. W.; Ayala, P. Y.; Morokuma, K.; Voth, G. A.; Salvador, P.; Dannenberg, J. J.; Zakrzewski, V. G.; Dapprich, S.; Daniels, A. D.; Strain, M. C.; Farkas, O.; Malick, D. K.; Rabuck, A. D.; Raghavachari, K.; Foresman, J. B.; Ortiz, J. V.; Cui, Q.; Baboul, A. G.; Clifford, S.; Cioslowski, J.; Stefanov, B. B.; Liu, G.; Liashenko, A.; Piskorz, P.; Komaromi, I.; Martin, R. L.; Fox, D. J.; Keith, T.; Al-Laham, M. A.; Peng, C. Y.; Nanayakkara, A.; Challacombe, M.; Gill, P. M. W.; Johnson, B.; Chen, W.; Wong, M. W.; Gonzalez, C.; Pople, J. A. GAUSSIAN 03, Gaussian, Inc., Pittsburgh, PA, 2003.
32. Addinsoft (2012). XLSTAT 2012.1, Data analysis and statistics software for Microsoft Excel, http://www.xlstat.com. Paris, France.
33. N.O. Eddy, *Mol. Simul*. 35(5) (2010) 354.
34. N. O. Eddy, F. E. Awe, C. E. Gimba, N. O. Ibisi, E. E. Ebenso, *Int. J. Electrochem. Sci*. 6 (2011) 931.
35. N. O. Eddy, S. R. Stoyanov, E. E. Ebenso, *Int. J. Electrochem. Sci*., 5 (2010) 1127.
36. W. Li , Q. He, C. Pei , B. Hou. *Electrochimica Acta* 52 (2007) 6386.

37. P. Fuentealba, P. Perez, R. Contreras, *J. Chem. Phys*. 113 (2000) 2544.
38. N.O. Eddy, B.I.Ita, *Intern. J. Quant. Chem*. 2010; DOI: 10.1002/qua
39. K. Ramji, D.R. Cairns, S. Rajeswari, *Appl. Surf. Sci*. 254 (2008) 4483.
40. I.Lukovits, I. Bakó, A. Shaban, E. Kálmán, *Electrochimica Acta* 43 (1998) 131.
41. I.Lukovits, A. Shaban, E. Kalman, Russian *J. Electrochem*. 39 (2003) 177.